

Removal of Mixed Pesticides from Drinking Water System Using Surfactant-Assisted Nano-TiO₂

J. Senthilnathan · Ligy Philip

Received: 21 July 2009 / Accepted: 22 September 2009 / Published online: 13 October 2009
© Springer Science + Business Media B.V. 2009

Abstract The present study focused on the degradation of mixed pesticides using UV-induced photocatalytic degradation of lindane (1 α ,2 α ,3 β ,4 α ,5 α ,6 β -hexachlorocyclohexane), methyl parathion (*O,O*-dimethyl-*O*-4-nitrophenyl phosphorothioate), and dichlorvos (2,2-dichlorovinyl-*O,O*-dimethyl phosphate). Different grades of TiO₂ were prepared through the acid route (AR), alcohol route (AIR), and surfactant route (SR) and their photocatalytic activity were compared with commercially available Degussa P-25 TiO₂. The rate of degradation of pesticides was high for TiO₂ prepared through the SR compared to the other three catalysts. The crystalline structure and morphology of SR TiO₂ was identified with scanning electron microscope, energy dispersive X-ray analyzer, UV, and transmission electron microscope analyses and was compared with that of Degussa P-25 TiO₂. Degradation studies of individual as well as mixed pesticides were carried out. The intermediate formed during the photodegradation of methyl parathion, lindane, and dichlorvos were identified by gas chromatography–mass spectrometry analysis.

Keywords Methyl parathion · Lindane · Dichlorvos · Surfactant · Photocatalytic degradation · TiO₂

1 Introduction

Pesticides of different chemical nature are being used extensively for agricultural purposes all over the world. Migration of pesticides to groundwater and surface water has become an issue of great concern as numerous incidents of contamination have been documented in developed countries (Mohammadi et al. 2006). Even when present in small quantities, their variety, toxicity, and persistence have an adverse effect on ecological systems such as birds, fish, and plants with which human welfare is inseparably bound (Gupta 2004). New methods for water treatment as well as improvements of the existing processes are essential to meet the stringent regulations that resulted from the increasing awareness about the adverse effects of these pollutants.

Methyl parathion (*O,O*-dimethyl-*O*-4-nitrophenyl phosphorothioate), dichlorvos (2,2-dichlorovinyl-*O,O*-dimethyl phosphate), and lindane (1 α ,2 α ,3 β ,4 α ,5 α ,6 β -hexachlorocyclohexane) are the most commonly used pesticides in India (Ma et al. 2003; Hoyer et al. 1998; Atiqur Rahman and Muneer 2005). Many researchers have reported the photocatalytic degradation of methyl parathion, lindane, and dichlorvos using TiO₂ in suspension form (Moctezuma et al. 2007; Evgenidou et al. 2007; Wang et al. 2007; Kim et al. 2006; Prakash et al. 2004; Zaleska et al. 2004; Evgenidou et al. 2005; Atiqur Rahman and Muneer 2005). Most of these studies focused on the degradation of a single pesticide in distilled water

J. Senthilnathan · L. Philip (✉)
EWRE Division, Department of Civil Engineering, Indian
Institute of Technology Madras,
Chennai 600036, India
e-mail: ligy@iitm.ac.in

system using aqueous TiO_2 suspension. However, in real-life conditions, a mixture of pesticides along with other organic compounds might be present. Moreover, there are several problems associated with using TiO_2 in suspension form such as requirement of an extensive solid–liquid separation process to separate the nano- TiO_2 particles from the drinking water system (Gelover et al. 2004). Hence, immobilizing TiO_2 on suitable support and employing this coated surface as the photocatalyst may be a promising solution for the above-mentioned problems (Gelover et al. 2004). Dionysiou et al. (2000) reported the degradation of lindane using TiO_2 immobilized on a continuous-flow rotating disk and achieved 63% of lindane degradation. The sol–gel method is considered as an effective approach for the preparation of immobilized TiO_2 films on various substrates (Shang et al. 2003; Chen and Dionysiou 2006).

TiO_2 in the anatase form appears to be the most photocatalytically active crystal phase compared to rutile (Adachi et al. 2004). Moreover, control of the morphology, particle size, particle size distribution, phase composition, and porosity of TiO_2 is vital to achieve optimum photocatalytic activity (Khanna et al. 2007). A variety of methods have been proposed for the preparation of nano- TiO_2 like flame synthesis, sol–gel routes, thermal hydrolysis, and reverse micro-emulsion method (Li-yuan et al. 2007). Among these techniques, a sol–gel thin film deposition offers several advantages over other techniques. The main disadvantage of sol–gel process is agglomeration of hydrolyzed TiO_2 particles (Mohammadi et al. 2006). Many methods have been developed to disperse the aggregated TiO_2 particles such as washing with organic solvent, freeze drying followed by heating, and adding surfactants (Li-yuan et al. 2007). The most economical and efficient way to prevent the aggregation of TiO_2 is the addition of surfactants. Surfactants are well known as stabilizers, template agents, and shape directors. Therefore, they have been adopted to realize controllable synthesis of nanoparticles. Highly photocatalytically active mesoporous TiO_2 with the particle sizes ranging from submicrometer to micrometer were synthesized using nonionic surfactants (Wang et al. 2007; Choi et al. 2006). The preparation of surfactant-assisted nano- TiO_2 microsphere showed better catalytic efficiency than Degussa P-25 TiO_2 (Zhang et al. 2009).

Very little work has been carried out on the degradation of mixed pesticides with immobilized TiO_2 . Most of the studies dealing with photocatalytic degradation of a single pesticide were carried out using Degussa P-25 TiO_2 . The present work is focused on the preparation of nano- TiO_2 by sol–gel process using acid, alcohol, and surfactant routes (AR, AIR, and SR, respectively). Nano- TiO_2 immobilized on Pyrex glass tube was employed to conduct photocatalytic degradation studies of methyl parathion, lindane, and dichlorvos. The photocatalytic activities of TiO_2 prepared by AR, AIR, and SR were compared with that of commercially available photocatalyst Degussa P-25 TiO_2 . Rates of degradation of lindane, dichlorvos, and methyl parathion were evaluated for individual and mixed pesticides using surfactant-assisted TiO_2 .

2 Materials and Methods

2.1 Chemicals

Analytical grade isopropanol (purity 99.7%) and ethyl alcohol (purity 99.9%) purchased from Ranbaxy Chemicals, India were used for the coating of titanium oxide nanoparticles. Methyl parathion, dichlorvos, and lindane of high-performance liquid chromatography (HPLC)-grade were also procured from Ranbaxy Chemicals, India, whereas methyl parathion, dichlorvos, and lindane of commercial grade (purity 80%) were purchased from the local market.

2.2 Preparation of Nano- TiO_2

Preparation of TiO_2 was carried out by three different methods using alcohol, acid, and surfactant.

2.2.1 Acid Route

For the preparation of acid-assisted (AR) TiO_2 , the colloidal solution was prepared according to the method suggested by Torimoto et al. (1997). Titanium isopropoxide (7.4 mL, 99% purity) was added dropwise to 30 mL of 1 M HNO_3 solution and agitated to give a transparent TiO_2 solution. The transparent solution was diluted with 100 mL of distilled water and the pH of the colloidal solution was adjusted to 3 using 1 M NaOH solution. The

suspension was agitated for 2 h at room temperature, centrifuged, and then washed with distilled water. The isolated TiO_2 was dried for 1 h at 100°C in a hot air oven. The resulting solid was calcined in a muffle furnace at 500°C .

2.2.2 Alcohol Route

For the preparation of alcohol-assisted (AIR) TiO_2 , a 0.1-M titanium isopropoxide solution in isopropyl alcohol was prepared and added to water in 1:1 ratio. The suspension was agitated for 1 h and centrifuged. The isolated TiO_2 was dried for 1 h at 100°C in a hot air oven. The resulting solid was calcined in a muffle furnace at 500°C .

2.2.3 Surfactant Route

The preparation of surfactant-assisted (SR) TiO_2 was carried out with hydrolysis of titanium isopropoxide in the presence of cationic surfactant (dodecyl amine). Titanium isopropoxide (0.4 M) was prepared in isopropanol and equimolar quantity of metal complexing agent acetyl acetone was added to it. The acetyl acetone forms complex with titanium and becomes golden yellow in color (Adachi et al. 2004). Dodecyl amine hydrochloride (0.4 M) in water was prepared by adjusting the pH to 4.5 with HCl. Both the solutions were mixed together and warmed up to 40°C until the mixture became transparent. The above solution was autoclaved up to 80°C for 72 h. The suspension was centrifuged at 8,000 rpm and residue was washed with alcohol for three times to remove the surfactant (Adachi et al. 2004; Sakulkaemaruethai et al. 2004). The dried sample was calcined at 500°C .

2.3 Immobilization of TiO_2

A Pyrex glass tube with an inner surface area of 169.56 cm^2 (with a height of 90 mm and a diameter of 60 mm) was used for coating the photocatalyst. Before coating, the inner surface of the Pyrex glass tube was treated with 5% (v/v) hydrofluoric acid for 30 min to get a rough surface and washed with distilled water. The Pyrex glass tube coating was carried out using different concentrations of TiO_2 and isopropanol suspension. Before coating, the suspension was sonicated for 15 min and the Pyrex tube was

inserted slowly into the suspension and allowed to stay in the suspension for 5 min, then taken out and dried in an oven for 30 min at 150°C . The weight of the coated materials was measured each time. The film thickness and surface morphology was also monitored.

2.4 Photoreactor

The schematic diagram of the photoreactor employed in the present study is given in Fig. 1. Photocatalytic degradation studies of methyl parathion, dichlorvos, and lindane were performed in an immobilized batch reactor. The cylindrical photochemical reactor with a volume of 400 mL was provided with water circulation arrangement to maintain the temperature in the range of $25\text{--}30^\circ\text{C}$. Irradiation was carried out with 125 W medium pressure mercury lamps supplied by Haber Scientific, India, which emitted predominantly UV radiation at a wavelength of 365 nm. For immobilized batch reactor, a coated Pyrex tube (inner surface area of 169 cm^2) was inserted into the reactor. Before adding the pesticide, the UV lamp was

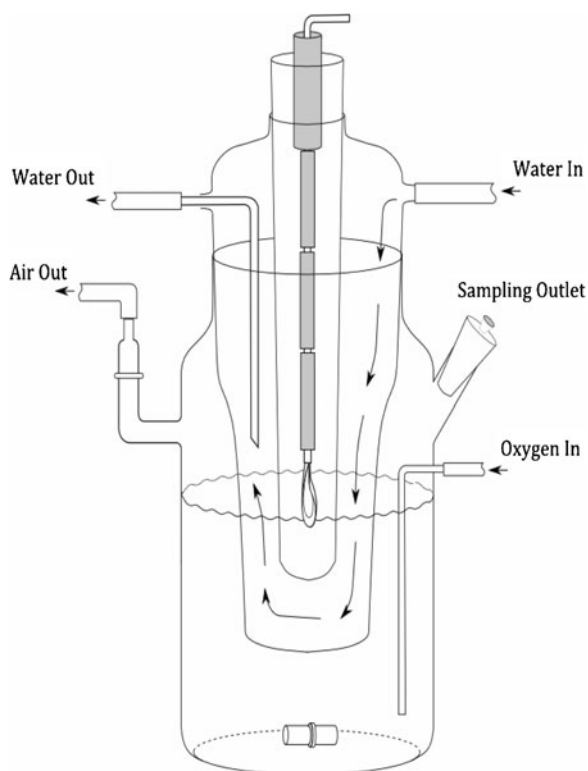


Fig. 1 Schematic diagram of photoreactor

warmed up for 15 min to attain sufficient energy. Oxygen flow rate of 300 mL/min and a stirring rate of 150 rpm were maintained in all the experiments. Samples were collected at regular intervals and extracted with HPLC-grade hexane (purity 99%) and analyzed using a gas chromatograph (GC) as mentioned earlier. The change in pH during the degradation of the pesticide was monitored with digital pH meter supplied by Digisun Electronics, India (model DI-707).

2.5 Analytical Methods

2.5.1 GC and GC-MS Analysis

Methyl parathion, dichlorvos, and lindane were analyzed using a Perkin Elmer Clarus 500 gas chromatograph with electron capture detector (GC/ECD) equipped with an autosampler, an on-column, split/splitless capillary injection system, and a Perkin Elmer (PE)-5 capillary column (30 m×0.53 mm×0.5 μm film thickness). The operating conditions were as follows: the column was initially held at a temperature of 80°C for 5 min and then the temperature was increased at a rate of 10°C/min to 180°C, followed by 8°C/min to 250°C and finally held at 250°C for 1 min. The temperatures of the injector and detector were maintained at 180°C and 350°C, respectively. Nitrogen was used as a carrier gas at a flow rate of 8.0 mL/min and the injections were made in the split mode with a split ratio of 1:10. The metabolites formed during the degradation were

monitored using a gas chromatograph–mass spectrometer (GC-MS) supplied by Agilent, USA, and a temperature program similar to the one used for GC analysis was employed for the GC-MS analyses also. Concentrations of NO_3^- , SO_4^{2-} , PO_4^{3-} , and Cl^- ions formed during the degradation of methyl parathion, dichlorvos, and lindane were analyzed using an ion chromatograph supplied by Dionex, USA with electrochemical detector (ED50).

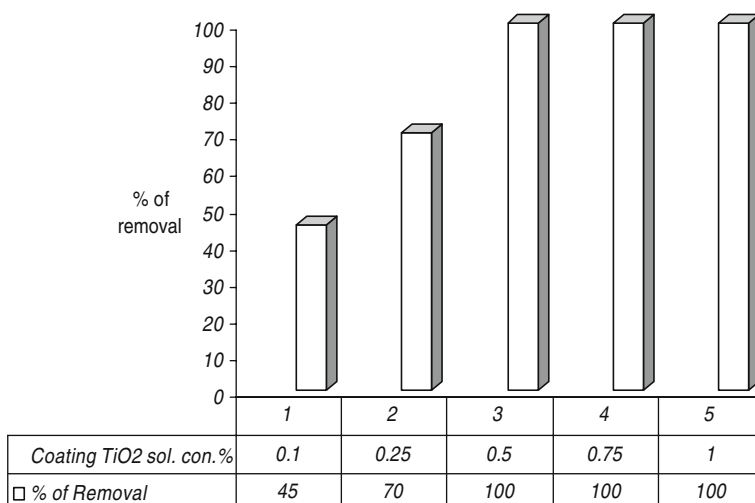
2.5.2 X-Ray Diffraction and UV Analysis

The crystalline structure of prepared TiO_2 was examined by X-ray diffraction (XRD) analyses, using Copper K alpha radiation with Lynx detector at an operating voltage of 35 kV and current of 25 mA supplied by Bruker Axs, USA (model D8 Discover). The Cary-5E UV–VIS–NIR, high-resolution spectrophotometer was used to find the absorption pattern of TiO_2 samples.

2.5.3 SEM, TEM, and EDAX Analysis

The surface morphology of the TiO_2 and particle size were determined using a scanning electron microscope (SEM) equipped with a field emission gun (JEOL, JSM-6380, Japan). The spot elemental analysis of synthetically prepared nano- TiO_2 and Degussa P-25 TiO_2 was carried out using SEM equipped with an energy dispersive X-ray analyzer (EDAX; FEI, Quanta 200, Czechoslovakia). High-resolution transmission electron microscope (TEM), JEOL 3010 with

Fig. 2 Effect of coating solution concentration on methyl parathion degradation



a UHR pole piece operating at an accelerating voltage of 300 kV, was used to measure the particle size of SR TiO₂.

2.6 Kinetic Studies

The kinetic study using SR TiO₂ was carried out with two different concentrations (1.0 and 2.5 mg/L) of methyl parathion, lindane, and dichlorvos. Coated TiO₂ was prepared separately for each study. Pseudo-first-order kinetic expression was used to analyze the photocatalytic reaction rate using the kinetic study data, and the kinetic expression is given by Eq. 1:

$$\ln(C_0/C) = kt \tag{1}$$

where *k* is the pseudo-first-order rate constant, *C* and *C*₀ are the concentrations at time *t* and *t*=0, respectively.

3 Results and Discussion

3.1 Effect of Coating Solution Concentration

Coating thickness is one of the important parameters in the performance of immobilized catalysts (Guillard et al. 2002). For effective degradation, TiO₂ should cover the entire area of the exposed reaction surface (Pyrex glass tube). TiO₂ suspensions with TiO₂ concentrations of 0.1%, 0.25%, 0.5%, 0.75%, and 1.0%, respectively, were prepared in isopropanol and used for coating the Pyrex glass tube. Preliminary

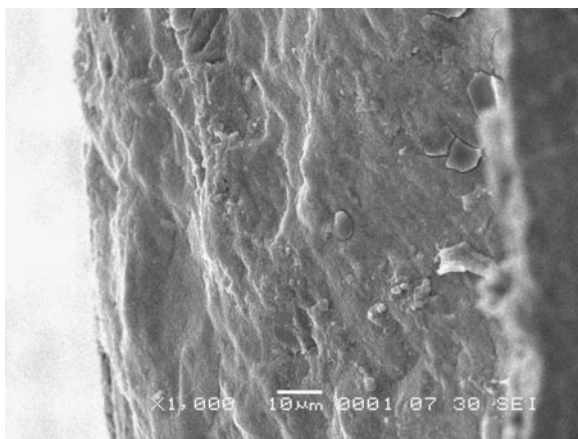


Fig. 3 Surface morphology of coated TiO₂

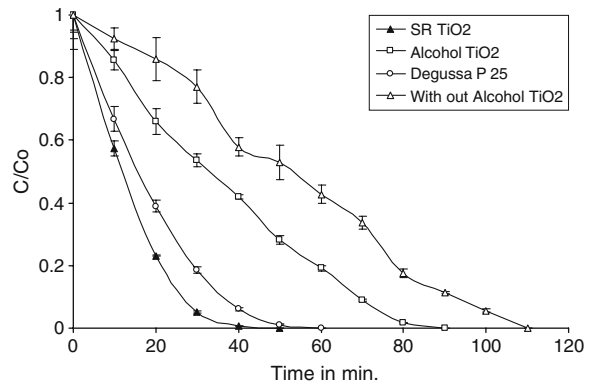


Fig. 4 Degradation of methyl parathion with different grades of SR TiO₂

degradation studies were carried out using 10 mg/L of methyl parathion with a reaction time of 60 min. The results are presented in Fig. 2. Methyl parathion was completely degraded in reactors which employed immobilized glass plates prepared using 0.5%, 0.75%, and 1.0% TiO₂ in isopropanol suspension solution. However, only 40% and 70% removals were attained in other reactors which employed 0.1% and 0.25% TiO₂ in isopropanol suspension for immobilization, respectively. Hence, 0.5% TiO₂ in isopropanol suspension solution was employed for immobilization in further studies. The weight of coated TiO₂ on Pyrex tube was monitored in each batch and it was around ~59±6 mg. The surface morphology of the coated Pyrex tube using 0.5% TiO₂ suspension is given in Fig. 3.

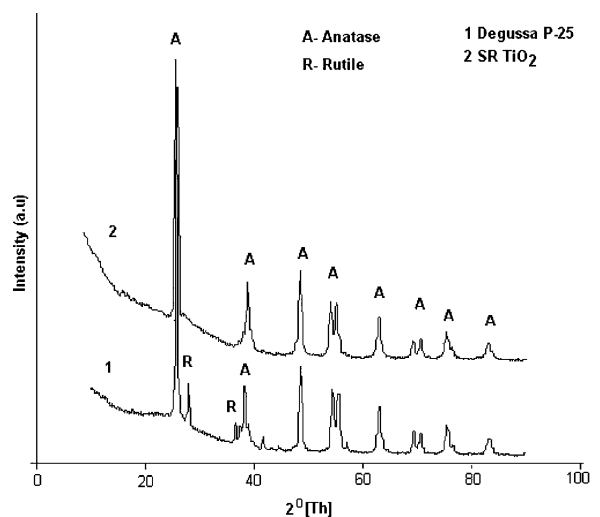


Fig. 5 XRD analyses of Degussa P-25 and SR TiO₂

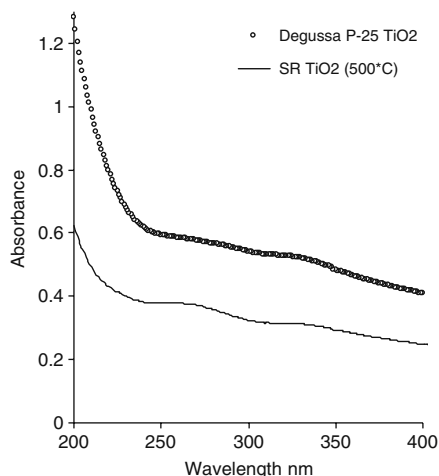


Fig. 6 UV-Vis spectrum of SR TiO₂

3.2 Screening of TiO₂ Prepared in Various Routes

The degradation of methyl parathion was carried out using three grades of TiO₂ immobilized on Pyrex glass tubes prepared through three different routes and the rates of degradation were compared with that of Degussa P-25 TiO₂. The results of methyl parathion degradation with different TiO₂ catalysts are presented in Fig. 4. Methyl parathion degradation efficiency was high for TiO₂ prepared through SR compared to the other three catalysts (Degussa P-25 TiO₂, AIR, and AR). Complete mineralization was achieved within 45, 55, 120, and 165 min for SR

TiO₂, Degussa P-25 TiO₂, AR TiO₂, and AIR TiO₂, respectively. The rate of degradation was dependent on particle size, crystalline structure and purity of the TiO₂. As SR TiO₂ performed better than other grades of TiO₂ during the screening study, this grade was selected for further studies.

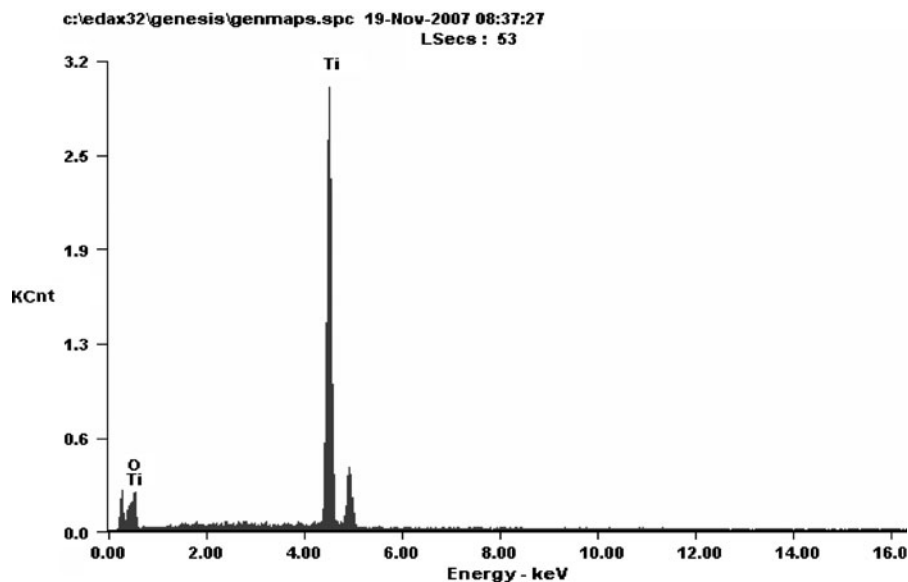
3.3 Characterization of SR TiO₂

3.3.1 X-Ray Diffraction and UV-Vis Spectra

The SR TiO₂ was dried in an oven at 500°C before it was used in the XRD analysis. The XRD patterns of TiO₂ were compared with those for Degussa P-25 TiO₂ and the results are given in Fig. 5. The strong XRD anatase peaks at $2\theta=25.4^\circ$ (101) and 48.0° (101) were observed in SR TiO₂ as well as in Degussa P-25 TiO₂. A strong rutile peak was observed at $2\theta=27.50^\circ$ in Degussa P-25 TiO₂, whereas a weak rutile peak was observed in SR TiO₂ at 54.5° (110). The XRD analysis showed a well-crystallized anatase peak and a weak rutile peak in SR TiO₂.

The UV-Vis spectra of SR TiO₂ (500°C) and Degussa P-25 TiO₂ were analyzed using 0.0025 M concentration of each catalyst and are given in Fig. 6. The absorption pattern of SR TiO₂ and Degussa P-25 TiO₂ indicated that the absorption was in the far UV region around 325 nm (3.85 eV). A similar UV absorption range, i.e., ~325 nm, for Degussa P-25 TiO₂ was reported earlier (Jwo et al. 2005).

Fig. 7 EDAX analysis of SR TiO₂



3.3.2 EDAX, SEM, and TEM Analyses

EDAX analysis was used to characterize the elemental composition of SR TiO₂. A typical EDAX pattern of SR TiO₂ is shown in Fig. 7. The elemental composition of oxygen and Ti were 38.21% and 60.79%, respectively. As per stoichiometric equation, titanium and oxygen in TiO₂ should be 59.9% and 40.06%, respectively. There was no other element found in the EDAX analyses. The particle size and morphology of TiO₂ catalyst were studied using SEM. It is clear from Fig. 8 that the size of the TiO₂ particles is approximately 30–50 nm. The exact sizes of the nanoparticles are very difficult to determine using SEM analysis; therefore, TEM analysis was carried out to find the exact size of the TiO₂ prepared through the SR (Gallezot and Leclercq 1994). From the TEM analysis, it was found that the particle size of SR TiO₂ is ~12 nm. Figures 8 and 9 show the SEM and TEM analysis of SR TiO₂.

3.4 Effect of Calcination Temperature on Photocatalytic Activity of SR TiO₂

Calcination improves the crystallization of TiO₂ powders and accelerates the transformation from the amorphous phase to the anatase or rutile phase (Zhang et al. 2000). Usually, beyond a calcination temperature of 500°C, strong rutile peak appears. The particle agglomeration is inversely proportional to its activation energy. It is reported that, when the calcination temperature is high, the activation energy is very low

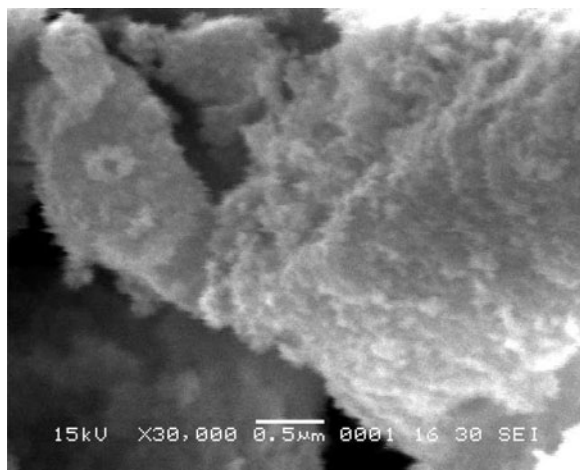


Fig. 8 SEM analysis of SR TiO₂

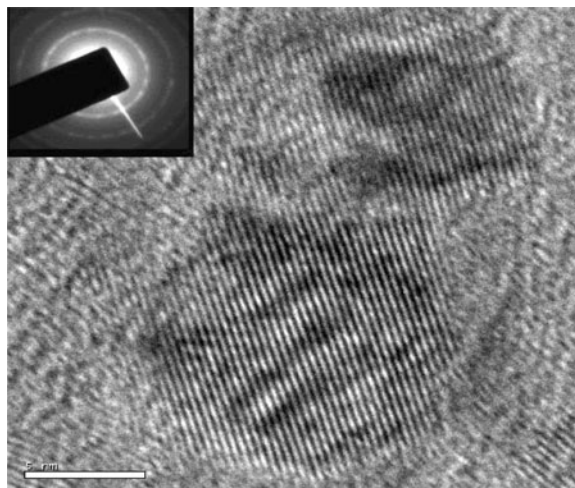


Fig. 9 TEM analysis of SR TiO₂

and the particle growth rate is large (Li et al. 2002). When the particle growth of TiO₂ increases, the catalytic activity decreases. Up to 500°C, the reduction in activation energy is very small (Li et al. 2002). Hence, in the present study, calcination temperature of TiO₂ was limited to 500°C. To find the optimum calcination temperatures, SR TiO₂ calcined at different temperatures (varying between 100°C and 500°C) and used for degradation studies. The XRD of SR TiO₂ prepared at different calcination temperatures are presented in Fig. 10. No anatase or rutile peak was observed for SR TiO₂ calcined at 100°C. As the calcination temperature increased beyond 200°C, sharp

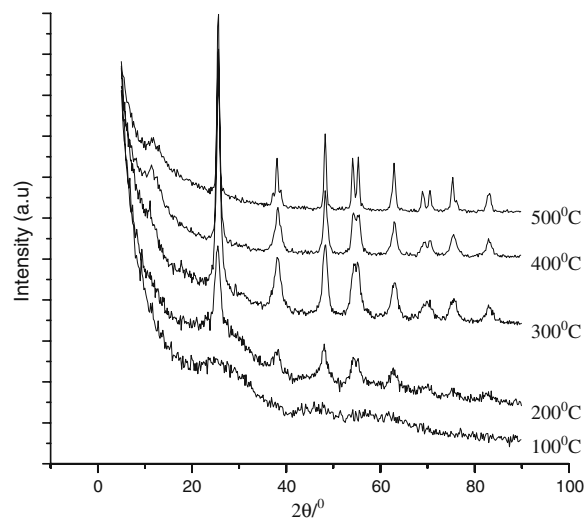


Fig. 10 XRD pattern of SR TiO₂ with different calcinations temperatures

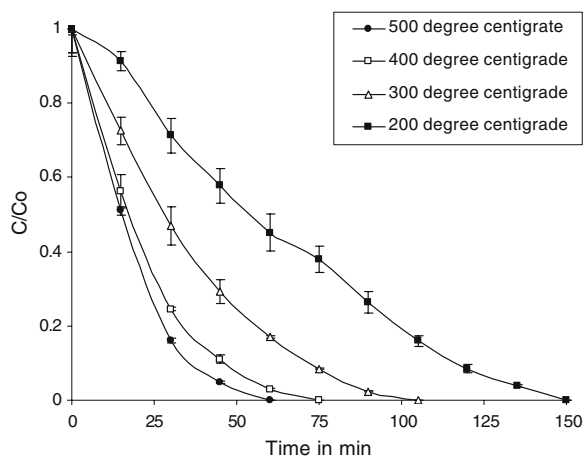


Fig. 11 Effect of temperature on catalytic activity of SR TiO₂

peaks of anatase and weak rutile peak started appearing. The degradation of methyl parathion (10 mg/L) with SR TiO₂ prepared at different calcination temperatures is given in Fig. 11. The photocatalytic activity of SR TiO₂ increased with increasing calcination temperature up to 500°C. A similar trend was observed for lindane and dichlorvos degradation also.

3.5 Effect of Pesticide Concentrations on Photodegradation by SR TiO₂

Degradation studies were carried out with two different concentrations (1.0 and 2.5 mg/L) of methyl parathion, dichlorvos, and lindane. The rate of degradation of methyl parathion, dichlorvos, and lindane was inversely affected by the initial pesticide concentration. A lower photodegradation rate was observed for lindane compared to methyl parathion and dichlorvos. This may be due to its high resistance to oxidation via hydroxyl radical attack. It is reported that lindane is less prone to oxidation due to its non-

aromatic and saturated structure and the absence of the double bond (Dionysiou et al. 2000).

The rate of degradation of the three pesticides was compared with Degussa P-25 TiO₂. The reaction rates, k (per minute), were determined by plots of $\ln(C/C_0)$ versus time for all the three pesticides and the results are given in Table 1. The rate of degradation of surfactant-assisted nano-TiO₂ was higher compared to Degussa P-25.

3.6 Plausible Degradation Pathways of Methyl Parathion, Dichlorvos, and Lindane

During the photocatalytic degradation of lindane, dichlorvos, and methyl parathion using SR TiO₂ as the photocatalyst, various organic intermediates were produced. Using the GC and GC-MS techniques, three by-products were identified during methyl parathion oxidation and five by-products were identified in the case of lindane oxidation. The degradation pathways of lindane and methyl parathion are given in Figs. 12 and 13. Only three intermediate by-products such as methyl paraoxon (m/z 246), *O,O*, *O*-trimethyl phosphonic thionate (m/z 156), and *p*-nitrophenol (m/z 139) were observed during the methyl parathion degradation. At the end of the reaction, methyl parathion and its by-products were completely degraded. Similarly, in the case of lindane degradation, hexachlorocyclohexane (m/z 289), pentachlorocyclohexane (m/z 256), hexachlorobenzene (m/z 284), 1-hydroxy-2,3,4,5,6-pentachlorobenzene (m/z 265), 1-hydroxy-2,3,4,5,6-pentachloro cyclohexane, and penta-hydroxyl cyclopentadiene (m/z 146) were identified. Most of the by-products appeared during the middle of the reaction and, as time progressed, the by-products gradually disappeared. Almost similar types of by-products were observed

Table 1 Reaction rate (k , per minute) and R^2 values for lindane, dichlorvos, and methyl parathion

Sample no.	Pesticides	Concentration (mg/L)	Degussa P-25 TiO ₂		SR TiO ₂	
			R^2	$k(\text{min}^{-1})$	R^2	$k(\text{min}^{-1})$
1	Dichlorvos	1.0	0.999	0.126	0.989	0.129
		2.5	0.987	0.104	0.987	0.112
2	Methyl parathion	1.0	0.998	0.136	0.998	0.141
		2.5	0.992	0.112	0.993	0.122
3	Lindane	1.0	0.994	0.016	0.992	0.018
		2.5	0.983	0.008	0.991	0.009

Fig. 12 Possible degradation pathway of methyl parathion by SR TiO₂

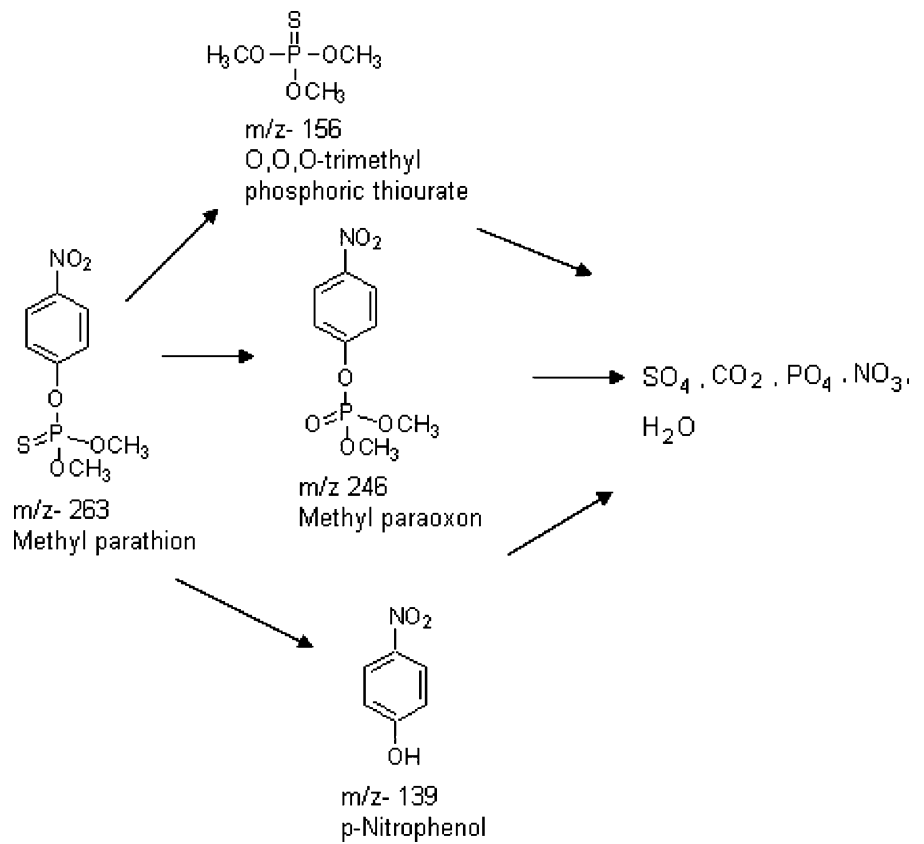


Fig. 13 Possible degradation pathway of lindane by SR TiO₂

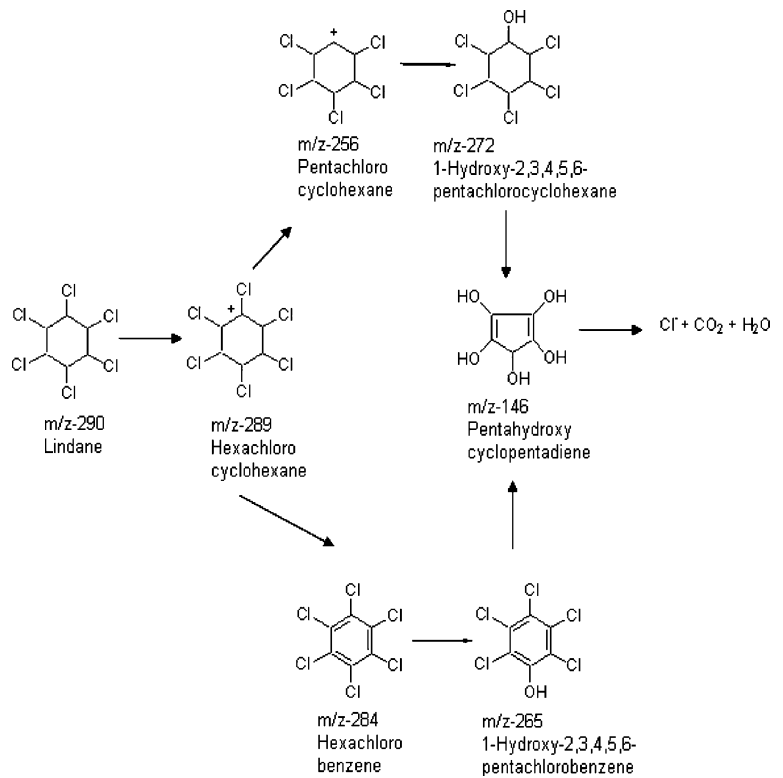


Table 2 Mineralization of lindane, methyl parathion, and dichlorvos

Sample no.	Free anion	Dichlorvos(mg/L)	Methylparathion(mg/L)	Lindane(mg/L)
1	Chloride (Cl ⁻)	2.75 (2.81)	–	5.36 (5.48)
2	Nitrate (NO ₃ ⁻)	–	9.11 (9.43)	–
3	Sulfate (SO ₄ ²⁻)	–	14.11(14.59)	–
4	Phosphate (PO ₄ ³⁻)	–	14.17(14.44)	–

The theoretical values of chloride, nitrate, sulfate, and phosphate are given in the bracket

during the degradation of dichlorvos, lindane, and methyl parathion with Degussa P-25 TiO₂. At the end of the experiment, none of the by-products were observed. In the case of dichlorvos degradation, no intermediate by-product was identified in GC-MS analysis.

To confirm the complete mineralization of pesticides, the end products SO₄²⁻, NO₃⁻, PO₄³⁻, and Cl⁻ were monitored during the degradation of all the three pesticides at regular time intervals. Methyl parathion degradation studies were conducted with an initial concentration of 40 mg/L and this amount of methyl parathion contains 14.59, 9.43, and 14.44 mg/L of SO₄²⁻, NO₃⁻, and PO₄³⁻, respectively. During methyl parathion degradation, removal of the sulfur group occurred first. A maximum concentration of 14.17 mg/L of free SO₄²⁻, 9.11 mg/L of free NO₃⁻, and 14.11 mg/L of free PO₄³⁻ were identified. A slight difference between theoretical and experimental values of SO₄²⁻, NO₃⁻, and PO₄³⁻ was observed. This may be due to the experimental and analytical errors. The concentration of chloride ions and change in pH during the degradation of lindane (initial concentration of 10 mg/L) and dichlorvos (initial concentration of 7.5 mg/L) were also monitored and the results are presented in Table 2. Chloride concentrations in the range of 2.79 and 5.36 mg/L were obtained for dichlorvos and lindane, respectively. The observed values were well in agreement with the stoichiometric concentrations of chlorides that can be generated from the given concentrations of pesticides.

3.7 Photodegradation of Mixed Pesticides

Photodegradation studies of mixed pesticides were carried out using identical mass concentrations of dichlorvos, lindane, and methyl parathion. Already, the attempt was made to photodegrade a high concentration of mixed pesticides (alachlor, atrazine, chlorfenvinphos, diuron, and isoproturon),

but complete mineralization was hard to accomplish (Maldonado et al. 2006). Therefore, a low concentration of (1.0 mg/L) mixed pesticides were employed for the photodegradation studies and all other experimental conditions were kept similar to the previous set of experiments. The results of the mixed pesticides degradation studies are presented in Fig. 14. Though degradation of all the three pesticide took place simultaneously, dichlorvos degradation was much faster compared to methyl parathion and lindane. Dichlorvos was completely degraded within 40 min, whereas 70 and 220 min were needed for the complete degradation of methyl parathion and lindane, respectively. Similar experiments were carried out with Degussa P-25 TiO₂; dichlorvos was completely degraded within 45 min, whereas 80 and 260 min were needed for the complete degradation of methyl parathion and lindane, respectively. The surfactant-assisted TiO₂ showed better catalytic efficiency compared to Degussa P-25 TiO₂ even in mixed pesticide systems. The GC and GC-MS analysis confirmed that there was no accumulation of intermediates in the system.

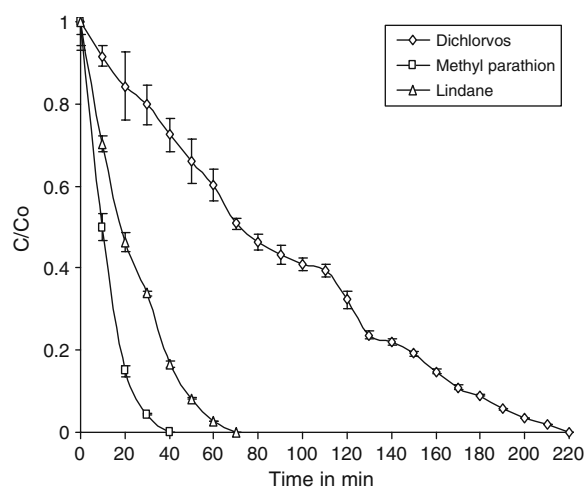


Fig. 14 Degradation of mixed pesticides by SR TiO₂ (C₀= 1 mg/L for individual pesticide)

4 Conclusion

The photocatalytic degradation of lindane, methyl parathion, and dichlorvos was studied using surfactant-assisted nano-TiO₂. The rate of degradation was high for TiO₂ prepared through the SR compared to that for TiO₂ prepared through AR and AIR and Degussa P-25 TiO₂. SEM and TEM studies showed that the particle size of SR TiO₂ was in the range of ~12 nm. The XRD studies showed the presence of strong anatase crystalline structure in SR TiO₂. EDAX analysis confirmed that the SR TiO₂ contains no impurities. GC-MS analysis showed that similar intermediates were identified for methyl parathion and lindane in single as well as mixed conditions. No reaction intermediate was identified during the degradation of dichlorvos. The rates of degradation of mixed pesticides were completely different from single pesticide.

References

- Adachi, M., Murata, Y., Takao, J., Jiu, J., Sakamoto, M., & Wang Highly, F. (2004). Efficient dye-sensitized solar cells with a titania thin-film electrode composed of a network structure of single-crystal-like TiO₂ nanowires made by the "Oriented Attachment" mechanism. *Journal of American Chemical Society*, *126*, 14943–14949.
- Atiqur Rahman, M., & Muneer, M. (2005). Photocatalysed degradation of two selected pesticide derivatives, dichlorvos and phosphamidon, in aqueous suspensions of titanium dioxide. *Desalination*, *181*, 161–172.
- Chen, Y., & Dionysiou, D. D. (2006). TiO₂ photocatalytic films on stainless steel: The role of Degussa P-25 in modified sol-gel methods. *Applied Catalysis B: Environmental*, *62*, 255–264.
- Choi, H., Stathatos, E., & Dionysiou, D. D. (2006). Synthesis of nanocrystalline photocatalytic TiO₂ thin films and particles using sol-gel method modified with nonionic surfactants. *Thin Solid Films*, *510*, 107–114.
- Dionysiou, D. D., Khodadoust, A. P., Kern, A. M., Suidan, M. T., Baudin, I., & Michel Laine, J. (2000). Continuous-mode photocatalytic degradation of chlorinated phenols and pesticides in water using a bench-scale TiO₂ rotating disk reactor. *Applied Catalysis B: Environmental*, *24*, 139–155.
- Evgenidou, E., Fytianos, K., & Poullos, L. (2005). Semiconductor-sensitized photodegradation of dichlorvos in water using TiO₂ and ZnO as catalysts. *Applied Catalysis B: Environmental*, *59*, 81–89.
- Evgenidou, E., Konstantinou, I., Fytianos, K., Poullos, I., & Albanis, T. (2007). Photocatalytic oxidation of methyl parathion over TiO₂ and ZnO suspensions. *Catalysis Today*, *124*, 156–162.
- Gallezot, P., & Leclercq, C. (1994). *Catalyst characterization: Physical techniques for solid materials*. New York: Plenum. Quoted by B. Imelik & J.C. Vedrine.
- Gelover, S., Mondragón, P., & Jiménez, A. (2004). Titanium dioxide sol-gel deposited over glass and its application as a photocatalyst for water decontamination. *Journal of Photochemistry and Photobiology A: Chemistry*, *165*, 241–246.
- Guillard, C., Beaugiraud, C. D., Herrmann, J. M., Jaffrezic, H., Renault, N. J., & Lacroix, M. (2002). Physicochemical properties and photocatalytic activities of TiO₂ films prepared by sol gel methods. *Applied Catalyst B: Environment*, *39*, 331–342.
- Gupta, P. K. (2004). Pesticide exposure—Indian scene. *Toxicology*, *198*, 83–90.
- Hoyer, A., Grandjean, P., Jorgensen, T., Brock, J. W., & Hartvig, H. B. (1998). Organochlorine exposure and risk of breast cancer. *Lancet*, *352*, 1816–1820.
- Jwo, C. S., Tien, D. C., Teng, T. P., Chang, H., Tsung, T. T., Liao, C. Y., et al. (2005). Preparation and UV characterization of TiO₂ nanoparticles synthesized by SANS. *Review on Advanced Material Science*, *10*, 283–288.
- Khanna, P. K., Singha, N., & Charan, S. (2007). Synthesis of nano-particles of anatase-TiO₂ and preparation of its optically transparent film in PVA. *Materials Letters*, *61*, 4725–4730.
- Kim, T., Kim, J., Choi, K., Stenstrom, M. K., & Zoh, K. (2006). Degradation mechanism and the toxicity assessment in TiO₂ photocatalysis and photolysis of parathion. *Chemosphere*, *62*, 926–933.
- Li, B., Wang, X., Yan, M., & Li, L. (2002). Preparation and characterization of nano-TiO₂ powder. *Materials Chemistry and Physics*, *78*, 184–188.
- Li-yuan, C., Yan-fen, Y., Gang, Z., Bing, P., & Shun-wen, W. (2007). Effect of surfactants on preparation of nanometer TiO₂ by pyrohydrolysis. *Transactions of Nonferrous Metals Society of China*, *17*, 176–180.
- Ma, T., Kramer, R. E., Baker, R. C., Fan, L. W., & Ho, I. K. (2003). Effects of chronic dermal exposure to nonlethal doses of methyl parathion on brain regional acetyl cholinesterase and muscarinic cholinergic receptors in female rats. *Journal of Neuroscience Research*, *71*, 138–145.
- Maldonado, M. I., Malato, S., Pérez-Estrada, L. A., Gernjak, W., Oller, I., Domenech, X., et al. (2006). Partial degradation of five pesticides and an industrial pollutant by ozonation in a pilot-plant scale reactor. *Journal of Hazardous Materials*, *138*, 363–369.
- Moctezuma, E., Leyva, E., Palestino, G., & de Lasa, H. (2007). Photocatalytic degradation of methyl parathion: reaction pathways and intermediate reaction products. *Journal of Photochemistry and Photobiology A: Chemistry*, *186*, 71–84.
- Mohammadi, M. R., Cordero-Cabrera, M. C., Fray, D. J., & Ghorbani, M. (2006). Preparation of high surface area titania (TiO₂) films and powders using particulate sol-gel route aided by polymeric fugitive agents. *Sensors and Actuators B: Chemical*, *120*, 86–95.
- Prakash, O., Suar, M., Raina, V., Dogra, C., Pal, R., & Lal, R. (2004). Residues of hexachlorocyclohexane isomers in

- soil and water samples from Delhi and adjoining areas. *Current Science*, 87, 73–77.
- Sakulkaemaruehai, S., Suzuki, Y., & Yoshikawa, S. (2004). Surfactant-assisted preparation and characterization of mesoporous titania nanocrystals. *Journal of the Ceramic Society of Japan*, 112, 547–552.
- Shang, J., Li, W., & Zhu, Y. (2003). Structure and photocatalytic characteristics of TiO₂ film photocatalyst coated on stainless steel webnet. *Journal of Molecular Catalysis A: Chemical*, 202, 187–195.
- Torimoto, T., Okawa, Y., Takeda, N., & Yoneyama, H. (1997). Effect of activated carbon content in TiO₂-loaded activated carbon on photodegradation behaviors of dichloromethane. *Journal of Photochemistry and Photobiology A: Chemistry*, 103, 153–157.
- Wang, J., Suna, W., Zhang, Z., Zhang, X., Li, R., Maa, T., et al. (2007). Sonocatalytic degradation of methyl parathion in the presence of micron-sized and nano-sized rutile titanium dioxide catalysts and comparison of their sonocatalytic abilities. *Journal of Molecular Catalysis A: Chemical*, 272, 84–90.
- Zaleska, A., Hupka, J., Wierowski, M., & Biziuk, M. (2004). Photocatalytic degradation of lindane, p, p DDT and methoxychlor in an aqueous environment. *Journal of Photochemistry and Photobiology A: Chemistry*, 135, 213–220.
- Zhang, Q., Gao, L., & Guo, J. (2000). Effects of calcination on the photocatalytic properties of nanosized TiO₂ powders prepared by TiCl₄ hydrolysis. *Applied Catalysis B: Environmental*, 26, 207–215.
- Zhang, X., Hong Pan, J., Du Jianhong, A., Ng, J., Darren, D., Sun, J., et al. (2009). Fabrication and photocatalytic activity of porous TiO₂ nanowire microspheres by surfactant-mediated spray drying process. *Materials Research Bulletin*, 44, 1070–1076.